Oceanologia (2018) 60, 500—512

Available online at www.sciencedirect.com

ScienceDirect

journal homepage: www.journals.elsevier.com/oceanologia/

ORIGINAL RESEARCH ARTICLE

Some characteristic wave energy dissipation patterns along the Polish coast

Grzegorz Różyński *, **Piotr Szmytkiewicz**

Institute of Hydro-Engineering, Polish Academy of Sciences, Gdańsk, Poland

Received 25 October 2017; accepted 10 April 2018
Available online 25 April 2018

KEYWORDS
Coastal morphology;
Wave energy dissipation;
Equilibrium profiles;
Data-driven modelling;
Signal processing

Summary The paper analyses cross-shore bathymetric profiles between Władysławowo (km 125 of the national coastal chainage) and Lake Sarbsko (km 174) commissioned in 2005 and 2011 by coastal authorities for monitoring purposes. The profiles, spaced every 500 m, cover beach topography from dune/cliff tops through the emerged beach to a seabed depth of about 15 m. They were decomposed by signal processing techniques to extract their monotonic components containing all major modes of the variability of beach topography. They are termed empirical equilibrium profiles and can be used for straightforward assessment of wave energy dissipation rates. Three characteristic patterns of wave energy dissipation were thus identified: one associated with large nearshore bars and several zones of wave breaking; a second, to which the equilibrium beach profile concept can be applied; and a third, characterized by mixed behaviour. Interestingly, most profiles showed significant seabed variations beyond the nearshore depth of closure — this phenomenon requires comprehensive studies in future.

* Corresponding author at: Institute of Hydro-Engineering, Polish Academy of Sciences, Kościerska 7, 80-328 Gdańsk, Poland. Tel.: +48 58 5222907; fax: +48 58 5524211.
E-mail addresses: grzegorz@ibwpan.gda.pl (G. Różyński), P.Szmytkiewicz@ibwpan.gda.pl (P. Szmytkiewicz).
Peer review under the responsibility of Institute of Oceanology of the Polish Academy of Sciences.

ELSEVIER Production and hosting by Elsevier

https://doi.org/10.1016/j.oceano.2018.04.001

1. Introduction

The first concepts of beach equilibrium profiles were developed empirically by Bruun (1954), who assumed that cross-shore beach topography is basically a function of wave energy E supplied to the shore at a shallow-water group wave velocity c_g. Bruun then concluded that nearshore seabed configurations are best described by monotonic power functions:

$$h(x) = Ax^n. \tag{1}$$

In Eq. (1) h is the seabed depth at the offshore distance x from the shoreline, and the parameters A and n are empirical quantities.

The theoretical background of the equilibrium beach configuration in constant hydrodynamic regimes was developed by Dean (1976), who assumed a constant wave energy dissipation rate E_r across the entire surf zone. Other assumptions included sediment homogeneity along the profile (D_{50} = const), monochromatic waves, linear wave theory and a constant wave breaking index $\gamma = H\,h^{-1} = const$. As a result, the wave energy dissipation rate could be calculated by:

$$E_r = \frac{5}{16}\rho g^{3/2}\gamma^2 h^{1/2}\frac{dh}{dx}. \tag{2}$$

Wave energy dissipation disappears at the shoreline for $h(x = 0) = 0$, and the well-known Dean monotonic beach equilibrium power function emerges for E_r = const:

$$h(x) = Ax^{2/3}. \tag{3}$$

The coefficient A has a dimension of $[m^{1/3}]$ and is directly related to E_r:

$$A = \left(\frac{24E_r}{5\rho g^{3/2}\gamma^2}\right)^{2/3}. \tag{4}$$

In Eq. (4), g = 9.81 m s^{-2} is the acceleration of gravity, and ρ = 1000 kg m^{-3} is the specific gravity of water. The situation of constant wave energy dissipation is known as the saturated wave breaking regime. It reflects the situation in which constant hydrodynamic forcing produces an equilibrium seabed configuration.

The relationships between the coefficient A and physical parameters of beach sediment were first investigated by Moore (1982). Next, Dean (1987) related this coefficient to the sediment fall velocity w_s with the formula $A = 0.067\,(w_s)^{0.44}$. A similar contribution by Kriebel et al. (1991) produced another fairly straightforward relationship:

$$A \approx 2.25\left(\frac{w_s^2}{g}\right)^{1/3}. \tag{5}$$

A temporal dependence of beach equilibrium profiles was proposed by Pruszak (1993), who introduced a time-varying A in the form of a sum of components oscillating over time:

$$A(t) = \overline{A} + A_1 + A_2 + A'. \tag{6}$$

In this expression, $\overline{A}$ is the time-invariant component expressed through e.g. Eq. (5), A_1 represents long-term variations due to the migration of large bed forms or changes in sediment supply driven by long-term variations in the hydrodynamic background, A_2 accounts for seasonal variability, and A' corresponds to short individual events, such as storms. Periodic changes in the parameter describing the equilibrium profile can be presented as:

$$A(t) = \sum_{k=1}^{2} a_k \cos\left(2\pi\frac{t}{T_k} + \theta_k\right) + A'. \tag{7}$$

The periods T_k correspond to long (k = 1) and medium (seasonal) time scales (k = 2); the period T_1 was found to be approximately 27 years for the Polish coast.

A different refinement of the beach equilibrium theory was proposed by Inman et al. (1993), who assumed a model in which the offshore portion of the profile was treated independently of the inner bar-berm portion, and both portions were matched at the breakpoint bar. Such partitioning was justified by different forcing modes on either side of the breakpoint. Both portions were fitted well by Eq. (1), with $n \approx 0.4$ being nearly the same for the bar-berm portion and the outer portion, irrespectively of seasonal changes. In this way, changes in seasonal equilibriums could be manifested by self-similar displacements of the bar-berm and outer curves, driven by seasonal surf zone variations.

Bodge (1992) addressed two major shortcomings of previous formulations, namely the physically unrealistic offshore-infinite range of beach equilibrium profiles and the infinite slope at the shoreline. He proposed an exponential curve, asymptotically converging to the closure depth to describe the beach equilibrium profiles. This effort was further improved by Komar and McDougal (1994), who replaced the closure depth with a ratio of the shoreline beach slope S_0 to the empirical parameter k [m^{-1}] accounting for profile concavity:

$$h(x) = \frac{S_0}{k}\left(1 - e^{-kx}\right). \tag{8}$$

This model predicts asymptotic convergence to a depth of S_0/k metres for the shoreline beach slope of S_0, which can be established as a function of sediment grain size and wave parameters, or evaluated directly from profile measurements, so only the concavity parameter k should be least-square fitted to profile measurements.

Several alternative approaches have been proposed to tackle shoreline singularity. Larson and Kraus (1989) suggested a form that superimposed a planar shallow water component with an offshore Dean form. Özkan-Haller and Brundidge (2007) introduced a further modification to limit the influence of the planar component to shallow water. Perhaps the most advanced model was presented by Holman et al. (2014), who developed an equilibrium beach profile concept capable of accounting for (a) a finite shoreline slope, (b) a concave-up form in wave-dominated shallow waters and (c) an asymptotic planar slope in the far field:

$$h(x) = \alpha\left(1 - e^{-kx}\right) + \beta x. \tag{9}$$

This model requires three parameters: (a) the far-field slope β can be obtained directly from available bathymetric charts, (b) the shoreline slope can also be easily established using the expression $d(h = 0)/d(x = 0) = S_o + \alpha k + \beta$, and (c) the depth h should be known at some location x', which can be anywhere in the profile, but should be representative of the background, average profile depth, so it should best be a

point seaward of the active bar zone. This last parameter is therefore subjective to some extent, but is necessary to establish the second equation relating α and k: $h(x') = \alpha(1 - e^{-kx'}) + \beta x'$.

The conceptual simplicity and modelling robustness of monotonic beach equilibrium profiles resulted in their wide acceptance. In particular, the equilibrium profiles are used extensively in beach fill design studies and projects, see e.g. CEM (2008) Part III-3, or CEM (2008) Part V-4. The major underlying reason is that the complicated and nonlinear phenomena of wave energy dissipation are often intractable by most physical models, particularly in systems with multiple bars. It can be briefly explained as follows:

1) When waves are mild, the surf zone is narrow, and they break only over the innermost bar.
2) Higher waves begin to break over the 2nd bar; the surf zone now includes two bars, and the breakers can include a spilling or a plunging mode or both.
3) During heavy storms, the outer bars contribute to wave energy dissipation as well — the surf zone now includes 4 bars or more and is several hundred metres wide. Various combinations of spilling and plunging modes are then possible, resulting in very complicated longshore and cross-shore sediment transport patterns.
4) Variations of wave set-up and wind-driven storm surges (in a range of 1 m) further modify the breaking regimes during the build-up, peak and recession of storms.

The insufficient robustness of physical models to successfully deal with complex surf zone morphodynamic processes necessitates other types of instruments that can provide some insight into the evolution of complicated coastal bathymetries. One such solution was proposed by Różyński and Lin (2015), who developed the concept of empirical equilibrium profiles. These profiles originate from actual bathymetric measurements and are derived by extraction of their monotonic components, which usually contain more than 90% of overall profile variability. Empirical equilibrium profiles relax the core assumption of theoretical Dean-type equilibrium profiles, namely the constant wave energy dissipation rate in the entire surf zone. In addition, if an empirical equilibrium profile closely resembles the shape of a Dean function, it demonstrates that saturated wave breaking regimes can be encountered in reality, at least along some portion of the surf zone, usually closer to the shoreline.

The extraction of empirical equilibrium profiles from measured cross-shore seabed configurations can be done by two methods of intensive signal processing: Empirical Mode Decomposition (EMD), see Różyński and Lin (2015), or Singular Spectrum Analysis (SSA), see Różyński et al. (2001). The only constraint is the monotonicity of empirical equilibrium profiles. It is needed to secure the applicability of Eq. (2), in which changes in wave energy dissipation intensity are governed primarily by the 1st derivative of the empirical equilibrium profile and secondarily by the square root of that profile. The positive sign of the derivative is needed to sustain wave energy dissipation. This equation is very useful because the resulting rates of energy dissipation are continuous, smooth and can be easily computed. Moreover, departures from actual dissipation rates are not very significant, because the empirical equilibrium profiles usually contain more that 90% of profile variability.

The primary goal of the paper was to identify wave energy dissipation patterns along a fairly long coastal segment in Poland, stretching between the western breakwater of the Władysławowo harbour (km 125 of the national coastal chainage) and a beach east of Lake Sarbsko (km 174). Wave energy dissipation patterns were identified using the empirical equilibrium profile concept for two sets of geodetically fixed bathymetric profiles commissioned in 2005 and 2011 by coastal authorities for monitoring purposes. Special attention was given to evaluation of the resemblance between empirical and theoretical Dean profiles in areas where saturated wave breaking regimes are encountered. The second goal was to identify the offshore range of application of the wave energy dissipation concept. This was done upon the assessment of the nearshore closure depth, based on the reconstruction of past wave climates (1958–2001) and the comparison of the offshore convergence of the two bathymetries of 2005 and 2011 at the offshore limit of the littoral zone. An unplanned by-product of the study was the identification of significant seabed variations beyond the nearshore depth of closure. This phenomenon consisted in significant changes in recorded bathymetries after profile convergence along their fairly long section, located at depths greater than 10 m. Some mechanisms regarding the driving force of those variations were hypothesized, providing grounds for follow-up studies.

2. Data and methodology

Fig. 1 presents the Polish coast and shows both ends of the national coastal chainage at km 0 (border with Russia) and km 428 (border with Germany). It also presents the limits of the study area at km 125 and 174. The profile lines, surveyed in the study area in 2005 and 2011, are geodetically fixed and spaced every 500 m, providing a rich data base with almost 100 profiles sampled twice. Their cross-shore range covers the area from the dune/cliff crest down to a depth of 15 m or more; it normally measures more than 2000 m. The surveys were commissioned by coastal authorities for monitoring purposes, in compliance with the Coastal Protection Act of Parliament of 2003.

A significant onshore and offshore extension of the profile lines provides a perfect opportunity for the extraction of their key modes of variability with much greater precision, as the extensive coverage substantially reduces the so-called end effects that can distort the modes of variability near the onshore and offshore profile extremities. One of data-driven techniques used for the extraction of the modes of variability, well tested in coastal applications, is the Singular Spectrum Analysis (SSA), see Appendix. Extensive background information on this method and its application to beach surveys can also be found, e.g. in Różyński et al. (2001). In brief, it consists in evaluation of the covariance structure of each profile and the computation of the associated modes of variability, known as the reconstructed components. If the number of points in a profile is n, then the number of modes of variability should not exceed $\frac{1}{3}n$ to eliminate imprecise estimation of higher modes. The modes are ranked according to the portion of total signal (profile)

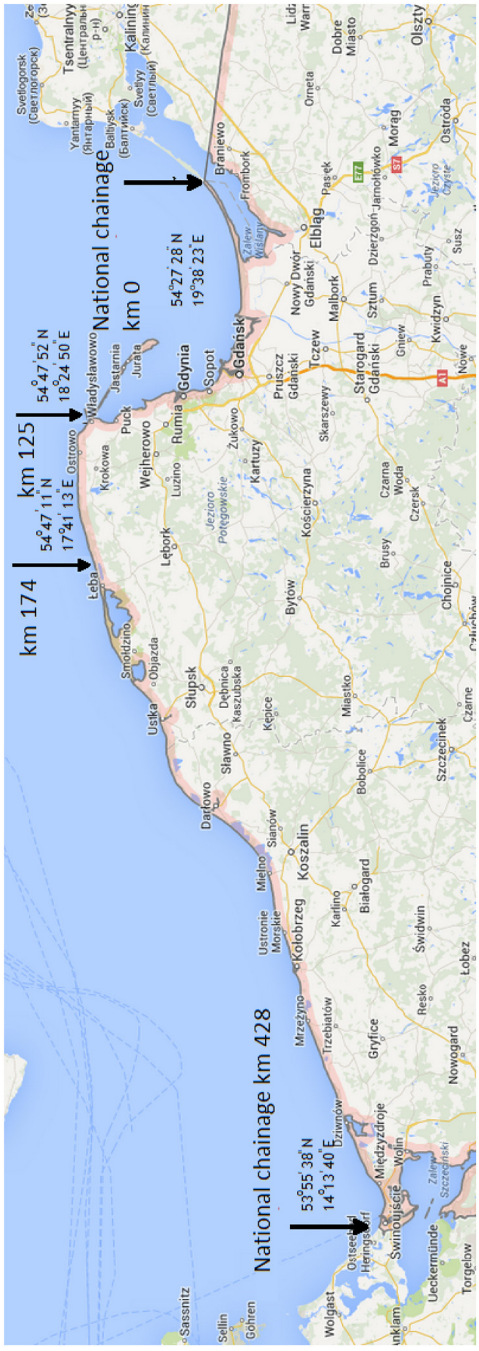

Figure 1 General map of Polish coastline.

variance each of them contains, starting from the one with the largest contribution. Being additive, they are summed, starting from the most significant one down to a mode whose inclusion destroys the monotonicity of the empirical equilibrium line. This summation is described in more detail for each profile line studied. The profiles studied usually contained 210—220 elements, so the maximum number of modes was set at $m = 70$. However, the number of modes that contribute to empirical equilibrium profiles was found to be much less, usually no more than 5.

3. Results

Fig. 2 shows fractions of profile variances explained by empirical equilibrium profiles for the survey of 2005. They were calculated for $N = 50$ profiles, so the span between the profiles was 1 km. The reason for that was twofold: (1) for a span of 500 m the profiles are often very similar, (2) computations of empirical equilibrium profiles for very similar profiles are usually redundant and do not add valuable information to the analysis. The average variance fraction explained by empirical equilibrium profiles was 92%, the related median 94.9%, the minimum 66.5% and the maximum 99.3%. On the basis of Fig. 2 we decided to scrutinize in detail 6 representative profiles whose explained variance is near the average value (km 130, 149 and 156) or significantly departs from that value (km 125, 139 and 161). These 6 profiles are marked in Fig. 2.

Fig. 3 presents the results of analysis for km 125. We can see that in both surveys the morphology is very similar and is dominated by two very large nearshore bars. Owing to the resemblance between the two surveys, SSA decomposition was done for the 2005 seabed configuration only. The empirical equilibrium profile contains only one mode of variability; the inclusion of another immediately destroys profile monotonicity. As a result, it significantly departs from the measured seabed configuration (see Fig. 2), as it contains only 73.7% of the original profile variability. This result demonstrates that the concept of one surf zone with wave breaking processes distributed continuously across its entire cross-shore range cannot be accepted, because the prominence of bars forms a beach system with intensive wave breaking processes along the offshore bar slopes and zones of no dissipation of wave energy inside the troughs. It was schematized by plotting three systems of coordinates, fixed at the shoreline and bar crests, for which separate Dean curves, representing disjoint subzones of wave energy dissipation, could be postulated. No saturated wave energy dissipation can be expected, though, and the monotonic profile cannot describe wave energy dissipation with sufficient precision.

Fig. 4 represents the analysis done for km 130 near Chłapowo, at the eastern end of a soft cliff running from Chłapowo to Jastrzębia Góra. Both surveys show one dominant bar with a crest situated about 400 m from the shoreline, which is preceded by a distinct trough with the greatest depth some 280 m offshore. The comparison of the two seabed configurations reveals substantial shoreline advance between 2011 and 2005 and much shallower depths onshore of the trough. The trough and the bar do not show important changes, and at a depth of some 7.5 m both profiles converge to the nearshore depth of closure.

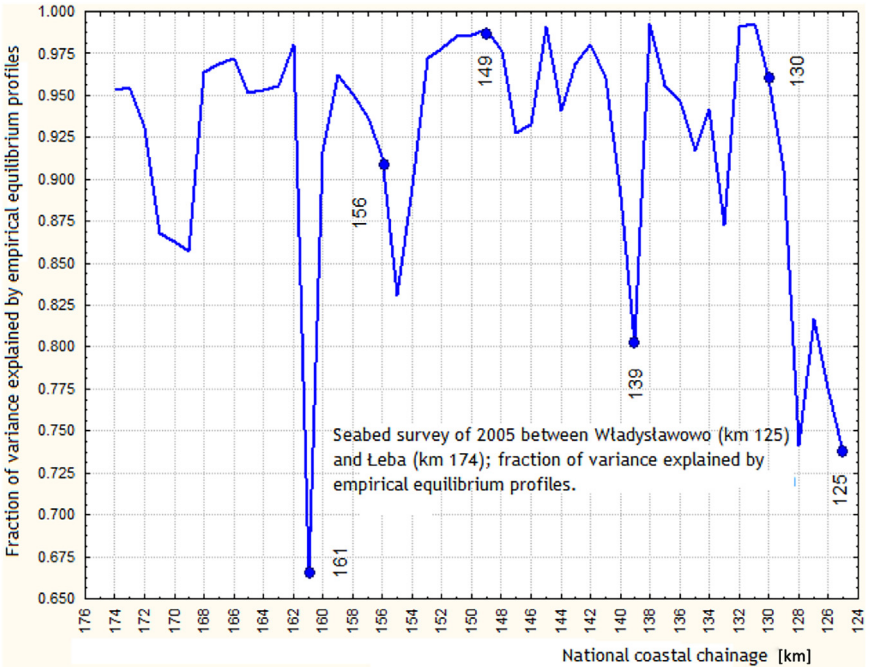

Figure 2 Fraction of profile variance explained by empirical equilibrium profiles.

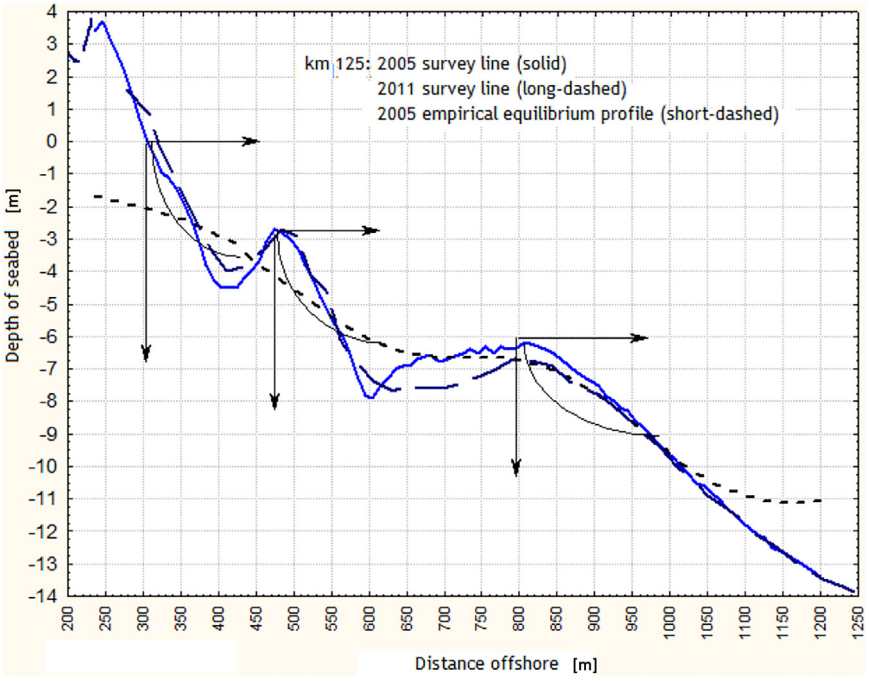

Figure 3 Empirical equilibrium profile at km 125.

The resemblance between the two surveys with respect to key morphologic features (locations and magnitudes of the bar and the trough) justified the computation of the empirical equilibrium profile for the seabed configuration of 2005 only. It consists of three modes of variability, which contain 96.1% of total survey variance. Thus, the empirical equilibrium profile reproduced the actual seabed configuration with high accuracy, highlighting the versatility of SSA decomposition. Its most important characteristic is the inflection point some 330 m offshore at a depth of about 3.5 m. The shape of the empirical equilibrium profile above that depth is akin to that of the Dean curve to a certain extent. Therefore, it can be assumed that the saturated wave breaking regime can develop there. The least-square fit of the Dean function to the empirical equilibrium profile yielded $A = 0.085\ \mathrm{m}^{1/3}$, and, using Eq. (4), the saturated rate of wave

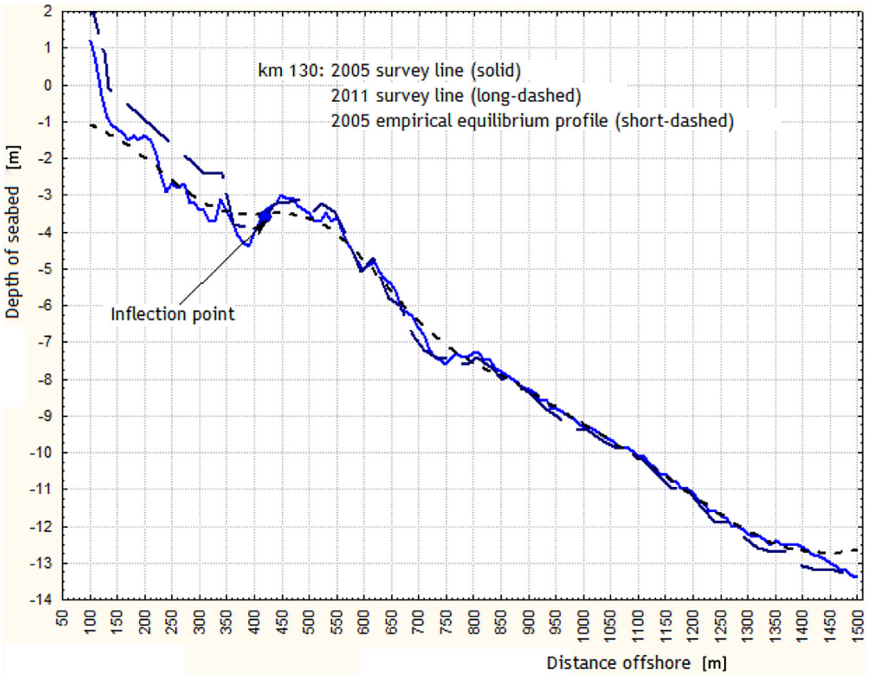

Figure 4 Empirical equilibrium profile at km 130.

energy dissipation was evaluated at E_r = 96.5 W m^{-2}. Offshore of that inflection point, seabed changes are not prominent and converge at about 7.5 m. Wave energy dissipation beyond the nearshore closure depth is negligible; it is initiated at that depth (7.5 m) and becomes saturated at 3.5 m. In all, the concept of saturated wave energy dissipation in the form of the beach equilibrium profile is fully applicable at km 130.

The next profile analyzed in detail is situated at km 139. Both surveys are plotted in Fig. 5. We can see that general morphological characteristics of the two surveys are the same, although in 2011 the bars and the shoreline moved onshore, so the beach underwent some erosion. Fig. 5 also shows the results of analysis. The profile at km 139 is located at Ostrowo, west of Jastrzębia Góra and east of Karwia. We can discern 5 nearshore bars, starting from the small innermost one, whose tiny crest is located at a depth of 1 m. The crests of the remaining 4 bars are located at 1.5, 2.1, 5 and 8 m. The empirical equilibrium profile consists of two modes of variability that embrace only 80.2% of the variance of the profile configuration of 2005. However, except for the offshore region of the outermost bar, absolute departures from the original seabed configuration are reasonable, so the empirical equilibrium profile is acceptable for multiple bars of moderate magnitude. Interestingly, the inflection point, similar to the one found at km 130, can be identified at a depth of 8 m. Moreover, its offshore distance is also the same as the offshore distance to the outermost bar, so they are both co-located. The remote location of the inflection point suggests that the entire surf zone morphology is close to the Dean-type regime of saturated wave breaking. The least-square fit of the Dean parameter to the empirical equilibrium profile yielded A = 0.089 and E_r = 103.4 W m^{-2}. The latter value closely resembles the saturated dissipation of wave energy at km 130 (96.5 W m^{-2}). Interestingly, the region of the outermost bar underwent the smallest seabed change, so it was justified to determine the depth of (nearshore) closure there. However, offshore of the rather flat and long crest of that bar, the two surveys diverged significantly on the offshore slope of the outermost bar at depths visibly greater than 8 m. This phenomenon was also found in other profiles and will be discussed later.

The next profile investigated in the current study is situated at km 149, just east of the mouth of the river Piaśnica, see Fig. 6. In 2005, it exhibited 3 shallow nearshore bars with crests at 0.5, 2 and 3.8 m. The related empirical equilibrium profile was composed of 4 modes of variability and matched very closely the 2005 survey line, capturing 98.9% of its variability There was also an inflection point at 4 m depth, just offshore of the 3rd bar (crest at 3.8 m). The fitted Dean parameter up to the inflection point was estimated as A = 0.086, and the related E_r = 98.2 W m^{-2}. In 2011, the two innermost bars merged into one quasi-bar structure. The smaller bar remained close to the location of bar 3 from 2005, with its crest at 3.8 m depth, located a bit onshore of the inflection point of the empirical equilibrium profile of 2005. The major difference between the surveys of 2005 and 2011 is a large trough found in the 2011 seabed morphology with a maximum depth of about 7.3 m, located about 450 m offshore. Further offshore, the seabed of 2011 exhibits a large outermost bar with the crest at 5.7 m depth and 650 m offshore. The related attempted empirical equilibrium profile retained 98.6% of total seabed variance, but lost monotonicity in the vicinity of the large trough. Thus, the profile at km 149 in 2011 exhibits two types of behaviour: one with the inflection point that delimits the zone of saturated wave breaking and a second, similar to km 125, where a large bar produces two subzones of wave breaking regimes. Consequently, this profile line demonstrates mixed behaviour: at times it generates conditions of saturated wave breaking and wave energy dissipation, whereas at other times it forms two separate zones of wave breaking and energy release.

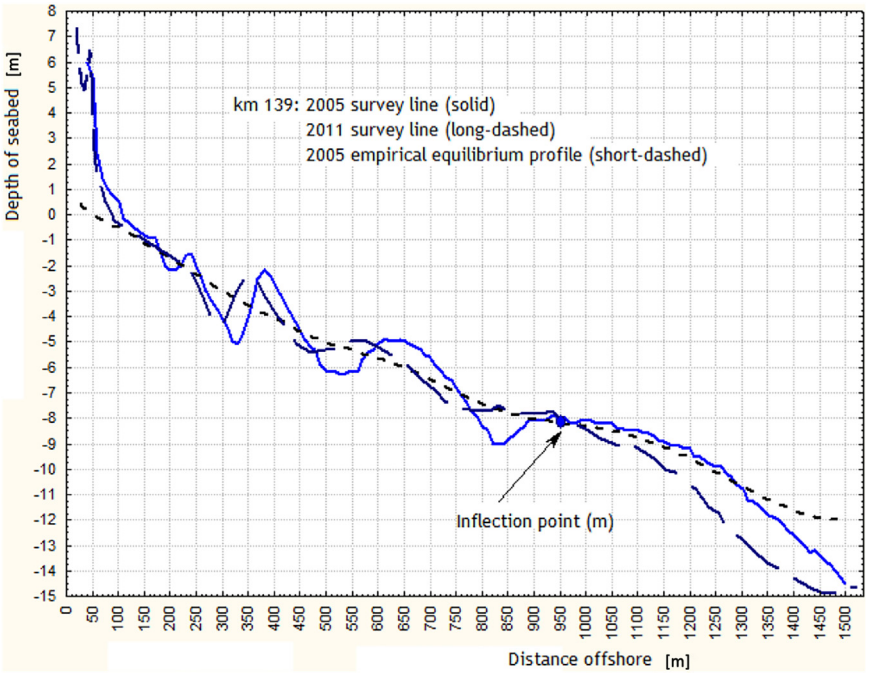

Figure 5 Empirical equilibrium profile at km 139.

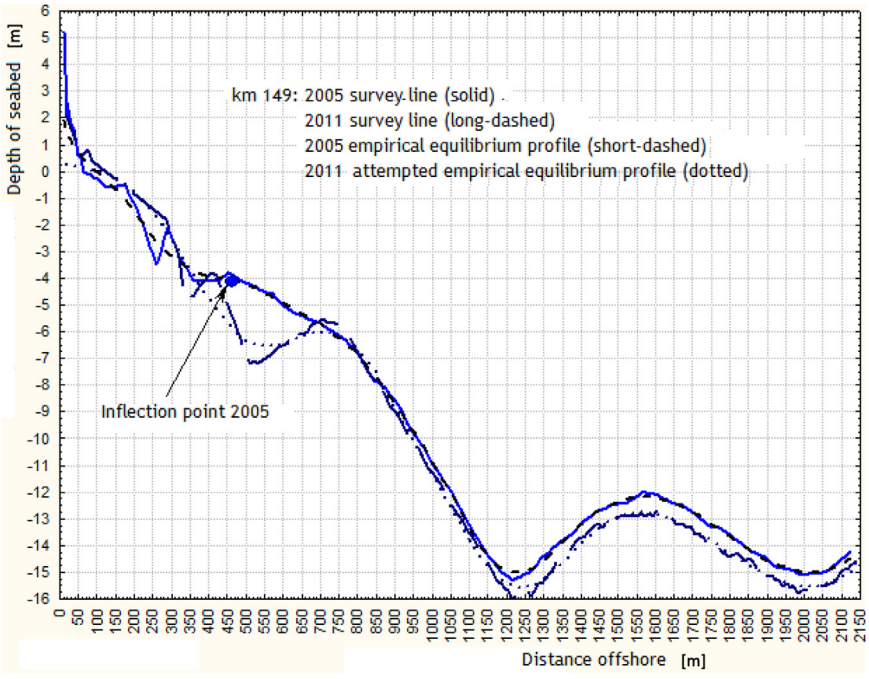

Figure 6 Empirical equilibrium profile at km 149.

Identification of mixed behaviour is a very strong point of SSA decomposition applied in the context of empirical equilibrium profiles. Interestingly, both profiles converge just offshore of the crest of the large bar at about 7 m depth, some 750 m offshore. This spot defines the (local) nearshore closure depth. The profiles remain close until some 1050 m offshore and 14 m depth. Then, they diverge, and the difference between the depths of the two surveys can reach 1 m.

The next profile is located at km 156 near Białogóra, see Fig. 7. In 2005, 3 tiny shallow bars were found at seabed depths of 2, 3 and 3.8 m. The associated empirical equilibrium profile has an inflection point in this region, at a depth of about 3 m and embraces 91.4% of the seabed variance of 2005 in 4 most significant modes of variability. The least-square fitted Dean parameter for this region was found to be $A = 0.069$, which corresponds to $E_r = 70.6\ \mathrm{W\ m^{-2}}$. This value points to a lower wave energy dissipation compared with the

previously analyzed configurations. The seabed in 2011 had some similarities to the profile from 2005, with bar crests at 1.9, 3 and 5.1 m. The main difference were three deep troughs found in 2011 at 3.5, 5.3 and 5.7 m. As previously, the two profiles converged at about 650 m offshore and opened up again at 900 m with depth discrepancies of over 1 m; the former location corresponds to the nearshore closure depth of 5.5 m. The empirical equilibrium profile for 2011 is plotted as the dotted line in Fig. 7. It contains 93.3% of seabed variance in 4 primary modes of variability. It also has an inflection point at a depth of 5 m, but the zone of saturated wave breaking is wider; the corresponding Dean parameter is $A = 0.083$, and E_r W m^{-2}. We can see that the zone of saturated wave energy dissipation can persist between measurements separated by as long as 6 years, but energy dissipation itself and the width of saturated energy dissipation can vary. However, it can be tentatively concluded that saturated wave energy dissipation decreases to 70—100 W m^{-2}. These results again underline the versatility of the empirical equilibrium concept and show variations of wave energy dissipation rates at the same site over semi-decadal scales.

Perhaps the most peculiar seabed configuration was discovered at km 161, see Fig. 8. This profile line runs through the submerged region of the Białogóra dune, whose onshore part was stabilized by forestation in the early 20th century. It is characterized by an enormous, remotely located bar, with the crest at some 900 m offshore at a depth of only 4.9 m. By contrast, the trough, located onshore, had a very large maximum depth of almost 11 m at some 600 m offshore. Closer to the shoreline, three typical smaller bars were discovered with crests at depths of 1, 2 and 3.5 m. The empirical equilibrium profile contained only one mode of variability that captured just 61% of signal variations. The line plotted in Fig. 8 has two modes of variability embracing 91.7% of total variability, but it significantly departs from monotonicity. This attempted empirical equilibrium profile points to behaviour similar to that found at km 125. The concept of saturated wave breaking is not applicable to this seabed configuration; there are definitely two zones of wave energy dissipation and saturation.

In 2011, the seabed configuration at km 161 was somewhat more typical. The huge bar moved offshore, so its crest shifted to 1100 m offshore and sank to a depth of 7 m, whereas the deep trough remained in place, but its depth decreased to 9 m. The other onshore bars remained more or less stable, the only difference being the shoreline retreat of about 50 m, which was not dangerous, because of the very wide beach. The attempted empirical equilibrium profile for 2011 turned out to be similar to that for 2005, except that it was generally much steeper. This was the result of the offshore translation and sinking of the huge outermost bar. In general, though, both seabed configurations represent a site in which a single zone of saturated wave breaking (and energy dissipation) is not possible. A relatively large time span between the two measurements (6 years) indicates that this situation is stable. Regarding the closure depth, both seabed configurations converged at a depth of 9.5 m, designating the offshore limit of the nearshore region, but diverged again at 13 m. This is another indication of a hydrodynamic forcing that is strong enough to trigger significant sediment motion at greater depths, beyond the nearshore region.

The above morphological findings require verification based on the available hydrodynamic data. One such dataset is the wave climate of the Baltic Sea reconstructed in the FP5 HIPOCAS project for the period of 1958—2001. A point near Lubiatowo located just offshore of the study area, for which such reconstructions were made, was therefore chosen to

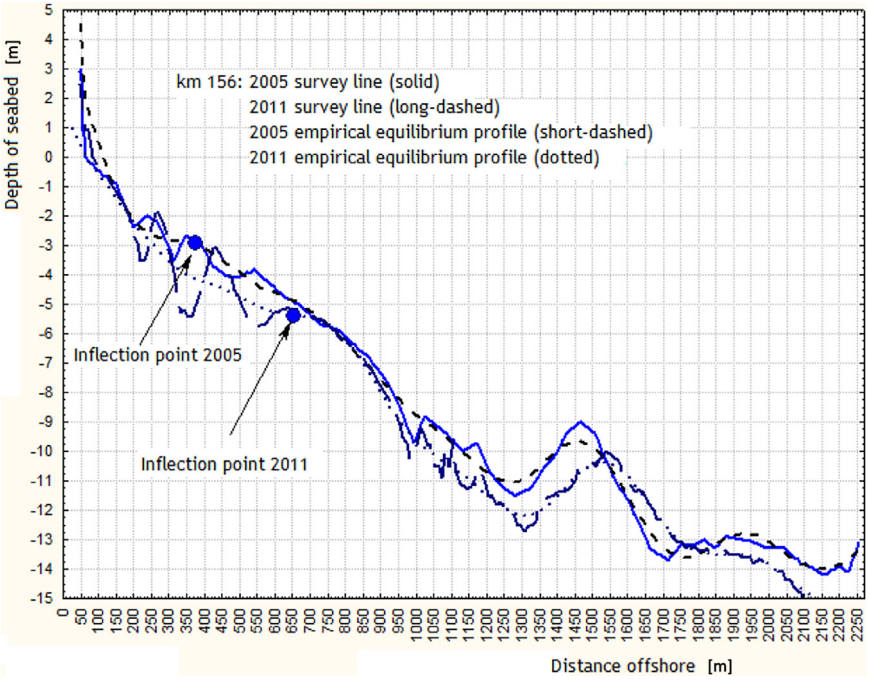

Figure 7 Empirical equilibrium profile at km 156.

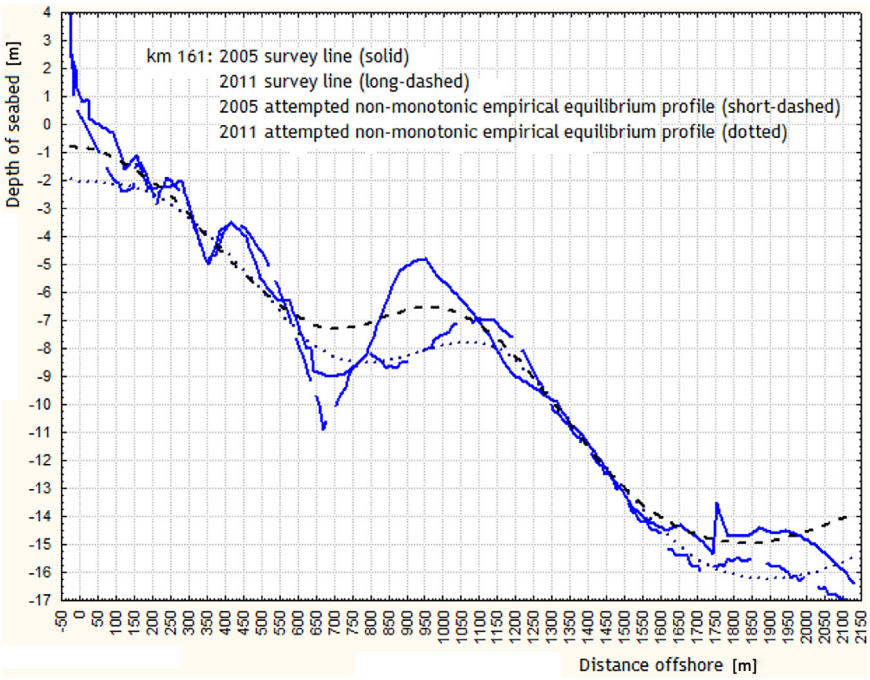

Figure 8 Empirical equilibrium profile at km 161.

Table 1 Statistical parameters of closure depth for 1958–2001 period (44 years).

Depth of closure parameters				
Mean [m]	Median [m]	Min [m]	Max [m]	St. Dev. [m]
8.4	8.2	5.9	10.7	1.15

calculate annual nearshore closure depths valid for all study area. Hallermeier's well-known formula was used, see Hallermeier (1981):

$$h_c = 2.28H_s - 68.5\left(\frac{H_s^2}{gT_s^2}\right). \tag{10}$$

In Eq. (10), H_s is a significant wave height exceeded for 12 h in the year preceding the seabed survey, and T_s is the associated wave period. The results are presented in Table 1. They were compared with the nearshore depths of closure of individual profiles between 2005 and 2011, put together in Table 2. We can see that the means and medians are very similar and range from 8 to 8.5 m. Thus, this value can be assumed as a fairly accurate estimate of the nearshore closure depth despite the fact that Hallermeier's estimates describe annual closure depths, whereas the investigations of seabed surveys span a period of 6 years. Both methods of estimating the nearshore closure depth also yield fairly low standard deviations, although the value obtained from comparisons of the two morphologies is roughly twice as high. The range between the minima and maxima is also greater for morphological observations. This cannot be surprising, because morphological considerations are based on very local profile characteristics, which vary significantly from site to site, whereas hydrodynamic data reflect wave climates valid for the entire study area.

Table 2 Statistical parameters of closure depths of individual profiles between 2005 and 2011.

Mean [m]	Median [m]	Min [m]	Max [m]	St. Dev. [m]
8.5	8.0	4	15	2.3

The relatively precise determination of the nearshore closure depth and identification of saturated wave breaking regimes at most beaches in Poland makes it possible to develop formulas for surf zone wave energy dissipation. We can assume that it is initiated at the nearshore closure depth and achieves saturation at the inflection point of empirical equilibrium profiles. In the most simplistic approach, wave energy dissipation outside the saturation sub-zone can be evaluated as:

$$E_r = E_{r_{dean}}\left[\frac{h_c - h}{h_c - h_{infl}}\right]^m \approx 100\left[\frac{h_c - h}{h_c - h_{infl}}\right]^m. \tag{11a}$$

In this equation, E_r represents wave energy dissipation between the locations of closure depth and inflection point. In other words, the saturation of wave energy dissipation develops between the nearshore closure depth h_c, where the expression in brackets is equal to zero, and the depth of inflection point h_{infl}, where it is equal to 1. Within the

Table 3 Descriptive statistical parameters of offshoremost bar and inflection point of empirical equilibrium profiles.

	Mean [m]	Median [m]	Min [m]	Max [m]	St. Dev. [m]
X_{infl}	472.9	425	100	925	212.7
X_{offb}	530	475	225	1050	240.7
h_{infl}	4.7	4.5	2.4	8.5	1.34
h_{offb}	4.4	4.3	2.1	8.5	1.37

sub-zone of saturated wave breaking, the formula reduces to $E_r = E_{r_{Dean}} \approx 100$ W m^{-2}. The cross-shore width of the zone with unsaturated wave energy dissipation is delimited by offshore locations of the nearshore closure depth X_c and inflection point X_{infl}. Eq. (11a) can be refined to include the actual profile configuration in the zone of unsaturated wave energy dissipation:

$$E = \frac{5}{16}\rho g^{3/2}\gamma^2 h^{1/2}\frac{dh}{dx}\left[\frac{h_c - h}{h_c - h_{infl}}\right]^m. \quad (11b)$$

The exponent m is normally set to 1. It can be further modified empirically if hydro-, litho- and morphodynamic observations and measurements provide sufficient justification. This estimation however is usually time-consuming.

One interesting aspect related to the locations of inflection points, determined by X_{infl} and h_{infl}, is their very high correlation with the corresponding locations of the outermost bar, given by X_{offb} and h_{offb}. The correlation between X_{infl} and X_{offb} is equal to 0.95, whereas for h_{infl} and h_{offb} the correlation is even greater and equals 0.97. This close relationship is further evidenced in Table 3, where basic statistical parameters of these four quantities are presented. We can see that inflection points should be located slightly deeper than the depth of the crest of the outermost bar and somewhat onshore of that crest. Thus, the location of the outermost bar may serve as a crude estimate of the location of the inflection points of empirical equilibrium profiles.

The last issue to discuss is the offshore divergence of profile surveys beyond their convergence at the nearshore closure depth. This phenomenon is not entirely unknown. It is widely accepted by offshore engineers that seabed evolution beyond the nearshore region can be significant. Hallermeier (1983) came up with the following formula:

$$h_{out} = 0.018 H_m T_m \sqrt{\frac{g}{D_{50}(s-1)}}. \quad (12)$$

In Eq. (12), H_m and T_m are the median wave height and period, respectively, D_{50} is the median sediment diameter, and s is the ratio of the specific gravity of sand to that of water (about 2.65). Formations of the offshore seabed can be attributed to earlier coastal and geologic processes, but not to the offshore movement of sediment from the present beach. The convergence of the profile envelope landward of those seabed formations indicates that sediment movement there is not directly related to sediment exchange in the nearshore profile.

Eq. (12) relates the mean wave conditions with D_{50}, a key sediment characteristic. Therefore, the average parameters of waves occurring over long periods of relatively calm weather are held responsible for seabed evolution beyond the littoral zone. This assumption can be realistic for the conditions of the United States, situated on two oceans, where wave lengths and periods are much longer than those recorded on the Baltic Sea. Nevertheless, the identification of significant seabed variations beyond the nearshore zone, after the apparent closure of seabed surveys at the nearshore closure depth h_c, demonstrates that the divergence of seabed surveys is also a common phenomenon in the Baltic Sea. For this reason, both components of Eq. (12) need to be verified for the Baltic Sea conditions. With regard to wave parameters, the available data can provide inputs for such analyses. However, energy fluxes related to mean waves in the Baltic Sea seem to be hardly sufficient to drive significant sediment movements beyond the nearshore zone for ordinary sands. Therefore, sediment samples from depths greater than about 14 m should be taken to obtain their granulometric curves, including D_{50}. Sufficiently small grains could justify the observed variations. However, it appears advisable to co-locate a current metre (or, better, an array of at least several current metres) in an area of sediment collection to obtain a full deepwater hydrodynamic background. The primary goal is to determine whether sufficiently strong oscillatory flows exist beyond the nearshore region. If they do, then Eq. (12) will be validated for the Baltic Sea conditions. However, if the oscillatory component is absent or insignificant, then the presently unidentified currents of other origin should be detected. Such currents can generate favourable conditions for non-trivial deepwater sediment motion, and Eq. (12) will have to be modified to include the current effect. This, however, is justified only when the hypothesized currents are actually detected.

One issue not discussed in this paper is the comparison of Dean coefficients obtained from least-square fits with those predicted by Hanson and Kraus (1989), who elaborated the relationships between A and D_{50} upon hydraulic experiments. Solution to this problem requires vast granulometric analyses of sediment samples from characteristic cross-shore locations in the surveyed profiles for a credible assessment of D_{50}. This is definitely a subject for follow-up research, which, however, requires an extensive field campaign.

4. Discussion

In general, the identified wave energy dissipation patterns are highly varied. For beaches with very large bars, whether natural or altered by anthropogenic activities, the concept of the equilibrium profile is not valid. In such instances, the surf zone consists of sub-zones, where energy dissipation occurs. Such zones are associated with offshore bar slopes that culminate at the crest. In troughs, often very deep, energy dissipation does not take place. Some assessment of energy dissipation intensity can be given by Eq. (2). Most profiles, though, exhibit zones of saturated wave breaking and energy dissipation, which can be identified when the empirical equilibrium profile is similar to the shape of the Dean function. Usually, such a zone starts at the shoreline and extends up to the inflection point. Interestingly, the evaluated maximum dissipation rates are in a range of about 100 W m^{-2}. The length of a segment where the saturated wave breaking regime and energy dissipation can develop and the associated dissipation intensity, are valuable pieces of information that can be used in beach fill design studies and procedures. Importantly, equilibrium conditions were reproduced from empirical measurements in areas where bars are not very large, and such systems can often exhibit erosive tendencies, particularly under changing climatic conditions. Therefore, they are usually subjected to beach fills, which are routinely designed on the basis of the equilibrium profile theory. On the other hand, the study results show that sediment-rich systems that usually develop isolated sub-zones of energy dissipation between very large bars, serving

as sediment buffers, are not usually prone to erosion and therefore are not subjected to beach fill operations.

With regard to individual profiles, the study revealed that the concept of monotonic empirical beach equilibrium profiles cannot be recommended for coastal segments in which distinct, very large bars occur. Such systems can have either natural (km 161) or anthropogenic origin (km 125). For example, the region of Białogóra (km 161) is known for its enormous natural dune system, located in both the emerged and submerged parts of the coastal zone. The emerged part was stabilized by humans with a forest, whereas the submerged part became a huge natural sand reservoir. In contrast, the construction of the western breakwater of the Władysławowo harbour (km 125) resulted in the obstruction of the predominant west-to-east littoral drift. In such instances, the empirical equilibrium profile significantly departs from the measured seabed configuration. The empirical equilibrium profile typically includes only the basic deepening seabed trend, usually contained in the first reconstructed component. The addition of another immediately destroys the monotonicity of the empirical equilibrium profile, so wave energy dissipation cannot be evaluated with Eq. (2): application of this equation to the empirical profile flawed by substantial departures from the original seabed configuration will certainly produce unrealistic assessments of actual wave energy dissipation rates. In sum, this observation indicates a possible line of follow-up research aimed at the identification of parameters limiting the applicability of the empirical equilibrium profile theory. Such parameters should be sought first in the geometry of barred profiles and then in sedimentary characteristics of coastal segments under study and their hydro- and lithodynamic background. The determination of these characteristics requires full-scale field experiments focused on seawater level changes, wave transformation, wave driven currents and seabed variations during storms and post-storm recovery periods.

The seabed configurations near soft cliffs (km 130) regularly develop steeper profiles without bars or with only one bar. The equilibrium zone is narrow, but the empirical equilibrium profile is usually monotonic. Also, its departures from the measured seabed configurations are usually small, so empirical equilibrium profiles can be used for the assessment of wave energy dissipation. The saturation of dissipation processes is possible in the narrow sub-zone, where the empirical equilibrium profile resembles the Dean function. In general, the presence of one bar reflects general erosive tendencies of soft cliffs on open sea coasts, where wave energy fluxes are only gently reduced over a bar and shoaling seabed and then attack the cliff foot directly, particularly during storms.

In general, most beaches with multiple bars of ordinary magnitude demonstrate equilibrium properties over the entire system of bars. The bars cannot be very large, so the empirical equilibrium profiles reproduce well over 90% of profile variability. These results show that the empirical equilibrium profile theory is fully applicable to most coastal segments in Poland.

The equilibrium conditions are identified at locations where the shape of empirical equilibrium profiles closely resembles the theoretical Dean curve. Such profiles usually extend from the shoreline up to the inflection point, beyond which they become concave. The locations of the outermost bar can serve as a fairly accurate proxy for the locations of the inflection points of empirical equilibrium profiles. The close resemblance between theoretical and empirical equilibrium profiles confirms the correctness of beach fill design principles, which are based on the Dean-type equilibrium profile theory and applied where the natural bars cannot sufficiently suppress wave energy during storms and prevent local erosion. The results of computations of wave energy dissipation show that this dissipation is in the range of 100 W m^{-3} (per unit volume of water) or 100 W m^{-2} (per longshore distance of 1 m). Also, the study of nearshore closure depths found a close resemblance between the estimates of closure depths from wave parameters and beach surveys. This led to a modification of wave energy dissipation formulas to include the zone where dissipation is initiated from zero up to saturation, associated with the inflection point of the empirical equilibrium profile. Onshore of that point, the saturated (constant) energy dissipation regime can be assumed. Finally, significant profile variations were identified beyond the nearshore region. Research on the nature of nearbed hydrodynamic regimes in that area should be conducted in order to determine whether oscillatory flow regimes of wave origin can drive noteworthy seabed variations, or whether other hydrodynamic phenomena (currents?) should be sought. Elimination of wave action as the agent of morphodynamic evolution outside the nearshore region will immediately trigger the question about the drivers of those hypothetical currents. The possible processes might include events of intensive water exchange between the Baltic and the North Sea, affecting the entire Baltic region, wind set-up during extreme events and the associated changes in the water table due to rapid passages of low-pressure air masses from (south) west to (north) east, or up- and down-welling events. Combinations of these processes are also possible. Parallel granulometric studies of sediments sampled beyond the nearshore region should provide additional information on minimum nearbed water velocities needed to mobilize the sediment there.

Overall, the analysis demonstrated that the coastline exhibits highly variable morphologies in the longshore direction, resulting in the corresponding longshore variations of wave energy dissipation rates. The monotonic empirical equilibrium profiles, made up of the sum of the modes of variability of SSA decomposition proved to be remarkably versatile and allowed us to determine highly variable wave energy dissipation rates. They can be divided into three basic classes: (1) this class includes the areas where wave breaking is relatively cross-shore uniform (km 130, 139 and 156), (2) locations where two or three sub-zones of intensive breaking exist (km 125 and 161), separated by deeper calm areas, in which broken waves can reform, and (3) locations of mixed behaviour (km 149), where sometimes predominantly cross-shore uniform wave energy dissipation rates can be observed and at some other times two distinct sub-zones of more intensive breaking can be encountered. This classification was achieved by the relaxation of the rigid assumption of constant energy dissipation, encapsulated in the Dean coefficient.

Acknowledgements

The research presented in this paper was financed and conducted under the H2020 project HYDRALAB+, contract number 654110 — HYDRALAB-PLUS — H2020-INFRAIA-2014—2015

and mission-related activities of IBW PAN, financed by the Polish Academy of Sciences.

Appendix. Singular spectrum analysis (SSA)

SSA is based on the Karhunen-Loéve expansion theorem, applied to the lagged covariance matrix of a time series x_i for $1 \le i \le N$. It has constant diagonals corresponding to equal lags:

$$T_x = \begin{bmatrix} c(0) & c(1) & \dots & c(M-1) \\ c(1) & c(0) & c(1) & . \\ . & c(1) & c(0) & . \\ c(M-1) & \dots & c(1) & c(0) \end{bmatrix}, \quad \text{(A1)}$$

where

$$c(j) = \frac{1}{N-j}\sum_{i=1}^{N-j}(x_i-\overline{x})(x_{i+j}-\overline{x}) \quad \text{(A2)}$$

and $\overline{x}$ is the mean value of the series. M is the user-defined *window length* or *embedding dimension:* the larger M is, the better the spectral resolution of oscillatory components in the time series. However, to reduce statistical errors in $c(j)$ for large lags j, it is recommended that M should not exceed $\frac{1}{3}N$.

The auto-covariance matrix is symmetric and positive definite for natural data, so the eigenvalues λ_k are positive, the eigenvectors E^k are orthogonal, and the scalar product of the (column) eigenvectors E^j and $E^l$is equal to the Kronecker delta:

$$\sum_{k=1}^{M} E_k^j E_k^l = \delta_{jl}, \quad 1 \le j \le M, 1 \le l \le M. \quad \text{(A3)}$$

The same is true for the scalar products of the jth and lth rows:

$$\sum_{k=1}^{M} E_j^k E_l^k = \delta_{jl}, \quad 1 \le j \le M, 1 \le l \le M. \quad \text{(A4)}$$

The eigenvectors are the invariant part of SSA decomposition and the variability is contained in *principal components* (PCs). The kth PC is a projection coefficient of the original signal onto the kth eigenvector:

$$a_i^k = \sum_{j=1}^{M} x_{i+j-1} E_j^k, \quad 1 \le i \le N-M+1. \quad \text{(A5)}$$

This equation states that we have to take M elements of the series x from the ith to $i + M$th element, compute their products with the corresponding elements of the kth (column) eigenvector and sum them up to obtain the ith element of the kth PC. Hence, the PCs are time series of the length $N-M$. Also, M consecutive elements of the series x are needed to compute one term of every PC, so there are k common elements of this series for the ith term of the rth PC a_i^r and the jth term of the sth PC a_j^s, such that $k = M-|j-i| > 0$ (lag $|j-i|$). Therefore, the correlation structure of the original series must be imprinted in the sequence of PC terms, producing non-zero correlations for non-zero lags.

The PCs do not provide a unique expansion of the signal: using the PCs, it can be expanded as:

$$x_{i+j} = \sum_{k=1}^{M} a_i^k E_k^j, \quad 1 \le j \le M. \quad \text{(A6)}$$

There may be up to M subsets of the original series containing the specific element x_{i+j}. Thus, there are up to M different ways of reconstructing the components of the signal with Eq. (A6), and a series having $N - M + 1$ elements is obtained. However, we can construct a least-square optimum series for a given subset of eigenelements by minimizing the following expression:

$$H_\Psi(y) = \sum_{i=1}^{N-M+1}\sum_{j=1}^{M}\left(y_{i+j} - \sum_{k\in\Psi} a_i^k E_j^k\right)^2, \quad \text{(A7)}$$

where y is the desired series, and Ψ is the subset of eigenelements. The solution is given by:

$$(R_\Psi x)_i = \frac{1}{M}\sum_{j=1}^{M}\sum_{k\in\Psi} a_{i-j+1}^k E_j^k \quad \text{for } M \le i \le N-M+1, \quad \text{(A8a)}$$

$$(R_\Psi x)_i = \frac{1}{i}\sum_{j=1}^{i}\sum_{k\in\Psi} a_{i-j+1}^k E_j^k \quad \text{for } 1 \le i \le M-1, \quad \text{(A8b)}$$

$$(R_\Psi x)_i = \frac{1}{N-i+1}\sum_{j=i-N+M}^{M}\sum_{k\in\Psi} a_{i-j+1}^k E_j^k \quad \text{for } N-M+2 \le i \le N. \quad \text{(A8c)}$$

If Ψ contains a single index k, the resulting series is the *k-th reconstructed component* (RC) x^k. The RCs are additive, so the series x can be *uniquely* expanded as the sum of its RCs:

$$x = \sum_{k=1}^{M} x^k. \quad \text{(A9)}$$

The RCs are then analyzed individually in terms of their magnitudes, trends, oscillatory behaviour and/or spells of chaotic behaviour with traditional signal processing tools. This process is the core of the SSA analysis. Usually, the whole useful information is contained in a few most significant RCs associated with the largest eigenvalues λ_k. They can be correlated, so the structure of correlations between the key RCs is frequently analyzed.

References

Bodge, K., 1992. Representing equilibrium beach profiles with an exponential expression. J. Coast. Res. 8 (1), 47–55.

Bruun, P., 1954. Coastal Erosion and Development of Beach Profiles. Tech. Memo. (Beach Erosion Board) No. 44, Washington, 1–79.

Coastal Engineering Manual (CEM) III-3, 2008. US Army Corps of Engineers, http://www.publications.usace.army.mil/Portals/76/Publications/EngineerManuals/EM_1110-2-1100_Part-03.pdf?ver=2014-03-10-134006-163.

Coastal Engineering Manual (CEM) V-4, 2008. US Army Corps of Engineers, http://www.publications.usace.army.mil/Portals/

76/Publications/EngineerManuals/EM_1110-2-1100_Part-05.pdf?ver=2014-03-10-135016-380.

Dean, R.G., 1976. Beach erosion: causes, processes and remedial measures. CRC Crit. Rev. Environ. Control 6 (3), 259—296.

Dean, R.G., 1987. Coastal sediment processes: toward engineering solutions. In: Proc. Coastal Sediments '87 Conf., American Soc. Civil Eng., New Orleans, LA, 1. 1—24.

Hallermeier, R.J., 1981. A profile zonation for seasonal sand beaches from wave climate. Coast. Eng. 4, 253—277, http://dx.doi.org/10.1016/0378-3839(80)90022-8.

Hallermeier, R.J., 1983. Sand transport limits in coastal structure design. In: Proc. Coastal Structures '83 Conf., American Soc. Civil Eng. 703—716.

Hanson, H., Kraus, N., 1989. GENESIS, Generalized model for simulating shoreline change. In: Technical Rep. CERC 89-19, Washington, USA, 1—185.

Holman, R.A., Lalejini, D.M., Edwards, K., Veeramony, J., 2014. A parametric model for barred equilibrium beach profiles. Coast. Eng. 90, 85—94, http://dx.doi.org/10.1016/j.coastaleng.2014.03.005.

Inman, D.L., Elwany, M.H.S., Jenkins, S.A., 1993. Shorerise and bar-berm profiles on ocean beaches. J. Geophys. Res. 98 (C 10), 18181—18199.

Komar, P.D., McDougal, W.G., 1994. The analysis of exponential beach profiles. J. Coast. Res. 10 (1), 59—69.

Kriebel, D., Kraus, N.C., Larson, M., 1991. Engineering methods for predicting beach profile response. In: Proc. Coastal Sediments '91 Conf., ASCE, Seattle, 557—571.

Larson, M., Kraus, N.C., 1989. SBEACH: numerical model to simulate storm-induced beach change. Tech. Re CERC-899, 115 pp.

Moore, B.D., 1982. Beach Profile Evolution in Response to Changes in Water Level and Wave Height. University of Delaware, Newark, USA, (MSc Thesis).

Özkan-Haller, H.T., Brundidge, S., 2007. Equilibrium beach profile concept for Delaware Beaches. J. Waterw. Port C Div. 133 (2), 147—160, http://dx.doi.org/10.1061/(ASCE)0733-950X.

Pruszak, Z., 1993. The analysis of beach profile changes using Dean's method and empirical orthogonal functions. Coast. Eng. 19 (3—4), 245—261.

Różyński, G., Larson, M., Pruszak, Z., 2001. Forced and self-organized shoreline response for a beach in the southern baltic sea determined through singular spectrum analysis. Coast. Eng. 43 (1), 41—58.

Różyński, G., Lin, J.G., 2015. Data-driven and theoretical beach equilibrium profiles: implications and consequences. J. Waterw. Port C Div. 141 (5), 04015002, http://dx.doi.org/10.1061/(ASCE)WW.1943-5460.0000304.